Pakistan Veterinary Journal

ISSN: 0253-8318 (PRINT), 2074-7764 (ONLINE)
DOI: 10.29261/pakvetj/2025.228

RESEARCH ARTICLE

Hycanthone inhibits African swine fever virus replication by inhibiting the cellular AKT phosphorylation and inducing viral DNA damage in porcine alveolar macrophage cultures

Zexin Liu[1,2], Yuanjia Liu[1], Guanming Su[1], Hui Li[1], Weixin Ou[1], Weisan Chen[3], Li Huang[4], Changjiang Weng[4,*], and Jianxin Chen[1,2,*]

[1]Guangdong Provincial Key Laboratory of Veterinary Pharmaceutics Development and Safety Evaluation, South China Agricultural University, Guangzhou, Guangdong 510642, China; [2]College of Veterinary Medicine, South China Agricultural University, Guangzhou, Guangdong 510642, China; [3]Department of Biochemistry and Genetics, La Trobe Institute for Molecular Science, La Trobe University, Melbourne, Victoria 3086, Australia; [4]Division of Fundamental Immunology, State Key Laboratory for Animal Disease Control and Prevention, Harbin Veterinary Research Institute of Chinese Academy of Agricultural Sciences, Harbin, 150069, China
*Corresponding author: wengchangjiang@caas.cn; jxchen@scau.edu.cn

ARTICLE HISTORY (25-553)

Received: June 14, 2025
Revised: August 07, 2025
Accepted: August 09, 2025
Published online: September 02, 2025

Key words:
African swine fever virus (ASFV)
Antiviral activity
AP endonuclease
Hycanthone
Porcine alveolar Macrophages (PAMs)

ABSTRACT

African swine fever (ASF), caused by ASF virus (ASFV) infection, is a highly contagious and severe hemorrhagic viral disease with significant economic implications for the global pig farming industry. Currently, there are no effective vaccines or antiviral drugs available for controlling ASF epidemics. Developing effective strategies to combat this epidemic has become imperative. In this study, by screening a chemical library with 400 small molecule compounds, we identified that hycanthone, a previously used anthelminthic drug, exhibits the most potent inhibition on ASFV replication in PAMs, with an IC_{50} value of 0.57 μmol/L. Hycanthone showed dose-dependent antiviral activity, reducing the mRNA levels of ASFV p30 and p72 proteins and decreasing viral DNA synthesis. Mechanistically, hycanthone attenuates ASFV replication by suppressing the cellular AKT phosphorylation and inducing viral DNA damage through interacting with ASFV AP endonuclease. Our findings suggest that hycanthone could serve as a promising therapeutic candidate for controlling ASFV infections.

To Cite This Article: Liu Z, Liu Y, Su G, Li H, Ou W, Chen W, Huangd L, Weng C and Chen J 2025. Hycanthone inhibits african swine fever virus replication by inhibiting the cellular AKT phosphorylation and inducing viral DNA damage in porcine alveolar macrophage cultures. Pak Vet J. http://dx.doi.org/10.29261/pakvetj/2025.228

INTRODUCTION

African swine fever virus (ASFV), an enveloped virus with an icosahedral morphology, is the sole member of the *Asfarviridae* family and possesses a double-stranded DNA genome ranging from 170 to 190 kbp (Nuanualsuwan *et al.*, 2022). It causes African swine fever (ASF), a devastating disease of domestic and wild pigs with profound economic impact. Since its initial identification in Kenya (1921), ASF has persisted globally for over a century (Gaudreault *et al.*, 2020). While eradicated in regions like Europe, the virus continues to spread elsewhere (L. Li *et al.*, 2022). The complex structure of ASFV has hindered the development of effective vaccines, underscoring the urgent need for antiviral drugs to control ASF outbreaks.

Recent studies have identified several natural compounds, including resveratrol, oxyresveratrol, and genkwanin, that exhibit antiviral activity against ASFV (Galindo *et al.*, 2011; Hakobyan *et al.*, 2019). Additionally, host-targeting compounds like dihydromyricetin (inhibiting TLR4-dependent pyroptosis) and brequinar (targeting DHODH) suppress ASFV replication (Grigoryan *et al.*, 2022; Chen *et al.*, 2023). Viral protein inhibitors such as enrofloxacin and genistein disrupt topoisomerase II activity essential for DNA topology (Freitas *et al.*, 2016; Arabyan *et al.*, 2018), while triapine and cyclabine hydrochloride target viral ribonucleotide reductase (pF334L) and pG1211R, respectively, impairing viral DNA synthesis (Li *et al.*, 2024). Despite these advances, no antiviral drugs have been approved for clinical use against ASFV, highlighting the need for continued research into novel therapeutic agents.

Hycanthone, an active metabolite of the anti-schistosomal agent lucanthone, was historically employed in the treatment of *Schistosoma mansoni* infections (Warren *et al.*, 1978). Its primary mechanism of action involves inhibition of RNA synthesis and DNA topoisomerase I/II activity, ultimately disrupting parasite

gene expression and DNA repair (Bases and Mendez, 1997). In addition to its well-established antiparasitic effects, hycanthone has also shown anti-inflammatory and antitumor activities in various experimental settings (Varbanov *et al.*, 2019; Boo *et al.*, 2023). However, little is known about its antiviral activity.

In this study, we screened a chemical library with 400 small molecule compounds, including AMPK activators, apoptosis and autophagy regulators, topoisomerase inhibitors, and endogenous metabolites, for their inhibition on ASFV replication in PAMs. We identified hycanthone as the most potent inhibitor of ASFV replication. Mechanistically, hycanthone inhibited viral replication by suppressing the cellular AKT phosphorylation and damaging viral DNA through interacting with ASFV AP endonuclease. Our findings suggest that hycanthone may serve as a potential antiviral agent against ASFV infections.

MATERIALS AND METHODS

Cell lines and virus strain: PAMs were isolated from 4–6-week-old ASFV-negative piglets under general anesthesia via lung lavage using ice-cold PBS containing penicillin/streptomycin, followed by centrifugation (800 × g, 10 min) and storage in RPMI-1640 medium at –196 ℃. The ASFV strain GZ201801 (GenBank: MT496893.1) was handled under biosafety level-3 conditions in South China Agricultural University (Guangzhou, China).

Cytotoxicity assay: Hycanthone (15 mmol/L) was dissolved in DMSO. Cytotoxicity was assessed via MTT assay: PAMs in 96-well plates were treated with serially diluted hycanthone for 48 h, incubated with MTT (0.5 mg/mL, 4 h), and dissolved in DMSO. Absorbance (570 nm) was measured to determine CC_{50} using GraphPad Prism 5.0 (Su *et al.*, 2024).

Indirect immunofluorescence assay (IFA): Cells were fixed, permeabilized, and blocked before incubation with anti-p30 or anti-p72 antibodies at 4 ℃ overnight. After PBS washes, cells were stained with AlexaFluor-conjugated secondary antibodies and DAPI. Images were captured using Leica fluorescence or confocal microscopes. Viral signals were quantified by fluorescence intensity in ImageJ and normalized to DMSO controls (Lim *et al.*, 2024).

Viral titer titration: PAMs seeded in 48-well plates (Corning Inc., USA) were infected with ASFV for 2 h at 37℃, and the medium was replaced with drug-containing maintenance medium. At 24 hpi, cellular and supernatant samples were harvested at specified intervals and processed through three iterative freeze-thaw cycles alternating between −80℃ and 4℃ to achieve complete virion liberation. The final viral titer was determined by the end point dilution assay using PAMs via IFA and was expressed as $\log_{10}$ $TCID_{50}$/mL (Liu *et al.*, 2021).

Quantitative real-time PCR (qRT-PCR, including qPCR and RT-qPCR): Viral DNA/RNA was extracted from cells sample using commercial kits (Fastagen, China). DNA was amplified with ASFV-p72 primers, while RNA was reverse-transcribed (Genstar, China) and amplified with ASFV-p30/p72 and GAPDH primers (Table 1). qRT-PCR used SYBR Green Master Mix (Genstar, China) on a Bio-Rad CFX96 system. Viral DNA copies were calculated from Ct values and mRNA levels ($2^{-\Delta\Delta CT}$ method) (X. Li *et al.*, 2022) were normalized to controls (DMSO-treated groups).

Table 1: List of primers used in this study.

Target	Sequences 5' to 3'	Orientation
ASFV-p72	GCAAAGACTGAACCCACTAATTT	Forward
ASFV-p72	TGTCATCATATTTGGCAGGTTT	Reverse
ASFV-RT-p30	TGCACATCCTCCTTTGAAACAT	Forward
ASFV-RT-p30	TCTTTTGTGCAAGCATATACAGCTT	Reverse
ASFV-RT-p72	ACGGCGCCCTCTAAAGGT	Forward
ASFV-RT-p72	CATGGTCAGCTTCAAACGTTTC	Reverse
PAMs-GAPDH	CCTTCCGTGTCCCTACTGCCAAC	Forward
PAMs-GAPDH	GACGCCTGCTTCACCACCTTCT	Reverse

Western blot analysis: Cell lysates (RIPA buffer) were centrifuged (15,000×g, 10 min, 4℃), and protein concentrations were determined via BCA assay. Proteins (10% SDS-PAGE) were transferred to PVDF membranes, blocked with 5% nonfat milk, and probed with anti-p72/p30, p-AKT, α-tubulin, or β-actin antibodies. HRP-conjugated secondary antibodies (1:5000) were applied (Beyotime, China), and signals were detected using Enhanced Chemiluminescence reagent (Han *et al.*, 2024).

Single cell electrophoresis analysis (comet assay): DNA damage was evaluated via alkaline comet assay: Cell samples were embedded in agarose, lysed, electrophoresed (300 mA, 25 min), and stained with propidium iodide. Tail DNA% was quantified using Comet Assay Software Project (CASP) in representative regions of three replicate slides for each sample (Li *et al.*, 2024).

Molecular docking: Molecular docking was conducted using SYBYL 7.3 (Wang *et al.*, 2023) with the ASFV AP endonuclease structure (PDB: 6ki3). Hycanthone's 3D structure was built in Discovery Studio and energy-minimized using CHARMm (Steepest Descent followed by Conjugate Gradient). Water molecules were removed before docking. Surflex-dock was used with 10 top hits and 10 random conformations. Compounds were ranked by –CDOCKER interaction energy.

Statistical analysis: All values are expressed as means ± SDs from at least three independent experiments. Statistical significance was determined by Student's *t*-test when only two groups were compared or by one-way analysis of variance (ANOVA) when more than two groups were compared. Statistical analyses were performed using GraphPad Prism 5 (GraphPad Software, San Diego, CA, USA). *P<0.05, **P<0.01 and ***P<0.001 were considered to be statistically significant at different levels.

RESULTS

Hycanthone inhibits ASFV infection in PAMs with low cytotoxicity: To identify compounds with anti-ASFV activity, we screened a library with 400 small molecules (10

μmol/L) by measuring changes in p72 DNA copies after compound treatment. The result showed that 12 candidates have significant anti-ASFV activity ($\Delta\log_{10}$ (p72 genomic copies)>0.5; Table 2), among which hycanthone demonstrated the most potent inhibitory activity against viral replication (Fig. 1A, B). Its chemical structure is shown in Fig. 1B. Cytotoxicity testing via MTT assay revealed that hycanthone was non-toxic to PAMs at concentrations below 15 μmol/L, with a CC_{50} of 21.7 μmol/L (Fig.1C). Dose-response analysis showed hycanthone inhibited ASFV replication in a concentration-dependent manner (Fig. 1D). The IC_{50} value was determined to be 0.57 μmol/L at 48 hpi, yielding a selective index (SI, CC_{50}/IC_{50}) of 38.

Table 2: The information of effective compounds.

Compounds	$\Delta\log_{10}$ (p72 genomic copies)	CAS number	Molecular formula
Danthron	0.60	117-10-2	$C_{14}H_8O_4$
Chitosan oligosaccharide	0.54	148411-57-8	
(+)-DHMEQ	0.70	287194-41-6	$C_{13}H_{11}NO_5$
Chloroquine	0.72	54-05-7	$C_{18}H_{26}ClN_3$
Saquinavir (Mesylate)	0.71	149845-06-7	$C_{39}H_{54}N_6O_8S$
Lonafarnib	0.94	193275-84-2	$C_{27}H_{31}Br_2ClN_4O_2$
Imatinib	0.54	152459-95-5	$C_{29}H_{31}N_7O$
Ancitabine	0.61	10212-25-6	$C_9H_{12}ClN_3O_4$
Kaempferol	0.74	520-18-3	$C_{15}H_{10}O_6$
Tizoxanide	0.62	173903-47-4	$C_{10}H_7N_3O_4S$
Amsacrine	0.59	51264-14-3	$C_{21}H_{19}N_3O_3S$
Hycanthone	1.38	3105-97-3	$C_{20}H_{24}N_2O_2S$

To confirm the anti-ASFV activity of hycanthone in PAMs, we assessed its effects on viral replication by measuring p72 DNA copies and p30 and p72 mRNA levels from 24 to 48 hpi. Hycanthone treatment markedly reduced p72 genomic DNA in a dose-dependent manner (Fig. 2A) and significantly suppressed transcription of early (p30) and late (p72) viral genes (Fig. 2B). Notably, exposure to 15 μmol/L hycanthone for 48 h resulted in a 99.5% decrease in p72 mRNA levels (Fig. 2B).

We further evaluated its inhibitory efficacy under different viral challenging doses. PAMs were infected with ASFV at 0.02, 0.2, or 2 MOI for 2 h, followed by treatment with 15 μmol/L hycanthone. Quantification at 24 hpi showed that hycanthone consistently inhibited ASFV replication across all doses, with over 90% reduction in p30 and p72 mRNA expression (Fig. 2C, D). Additionally, hycanthone's antiviral effect was confirmed by IFA and western blot analysis of p30 and p72 protein expression, further demonstrating its potent inhibition of ASFV replication in PAMs (Fig. 3).

Hycanthone suppresses ASFV replication in pre-, co- and post-treatment modes: To determine which stages of the ASFV life cycle were affected by hycanthone, PAMs were treated with hycanthone (3.75, 7.5, or 15 μmol/L) before (pre-treatment), during (co-treatment), or after (post-treatment) infection (Fig. 4A). At 24 hpi, ASFV p72 protein expression and viral DNA levels were assessed by IFA and qPCR, respectively. Pre-treatment for 3 h reduced p72 protein expression (Fig. 4B, C) and p72 genomic copies (Fig. 4H) in a dose-dependent manner, suggesting decreased cell susceptibility. Similar inhibition was observed in the co- and post-treatment groups. During co-treatment, 15 μmol/L hycanthone reduced p72 protein by 85% (Fig. 4E) and decreased p72 genomic DNA by 1.77 log (Fig. 4I). In the post-treatment mode, adding hycanthone at 6 or 12 hpi reduced p72 protein expression by 82% and 62%, respectively, whereas treatment at 18 hpi showed no effect (Fig. 4F, G). Consistent decreases in viral DNA were confirmed by qPCR (Fig. 4J). These findings demonstrate that hycanthone effectively inhibits ASFV replication at multiple stages of the viral life cycle.

Hycanthone inhibits viral attachment and internalization rather than viral release in PAMs: Since hycanthone exhibited the strongest inhibition in the post-treatment mode, we further investigated which stages of the ASFV replication cycle were affected. ASFV-infected PAMs were treated with 15 μmol/L hycanthone at different time points (Fig. 5A). Early treatments (0–6 h and 6–12 h) showed stronger inhibition than later ones (12–18 h and 18–24 h). Reductions in viral p72 protein expression were 95%, 83%, and 71% for treatments at 0–6 h, 6–12 h, and 12–18 h, respectively, while treatment at 18–24 h had no significant effect (Fig. 5B and 5C). Similar trends were observed in viral DNA levels by qPCR (Fig. 5D), indicating hycanthone mainly inhibits ASFV replication during the early and middle stages, rather than the late stage.

Given that virus binding and internalization occur early during infection, we next assessed whether hycanthone affects these steps. For attachment assays, PAMs were infected and treated with varying concentrations of hycanthone at 4℃ for 2 h. For internalization assays, cells were infected at 4℃, washed, and then incubated at 37℃ in hycanthone-containing medium (Fig. 6A). Hycanthone significantly inhibited both attachment (Fig. 6B, 6C) and internalization (Fig. 6D, 6E) in a dose-dependent manner. As ASFV replication completes around 24 h with progeny virus release at later stages (Salas and Andres, 2013), we also tested whether hycanthone impacts viral release by treating cells at 18–24 hpi. Results (Fig. 6F and 6G) showed hycanthone did not affect virus release into the medium. Together, these findings demonstrate that hycanthone inhibits ASFV primarily by targeting viral attachment, internalization, and early to middle replication stages.

Hycanthone exhibits inhibition on ASFV replication by inhibiting p-AKT expression: Activation of AKT is an early event in ASFV replication and is involved in viral entry (B. Yang *et al.*, 2023). Our findings show that hycanthone effectively inhibits early ASFV replication and blocks virus attachment and internalization, suggesting a role in AKT pathway suppression. Notably, hycanthone, like the AKT inhibitor LY294002, reduced p-AKT levels in both infected and uninfected PAMs (Fig. 7A, 7B). Moreover, AKT activation by insulin reversed hycanthone's inhibition of p-AKT and p30 expression (Fig. 7C, 7D). These results indicate that hycanthone's antiviral effect against ASFV is partly mediated through the AKT pathway.

Hycanthone suppresses the production of ASFV factories and induces ASFV DNA damage: ASFV forms virus factories in the cytoplasm to facilitate its replication, assembling structural proteins within these sites (Zhou *et al.*, 2022). The late protein p72, the major capsid protein, serves as a marker for ASFV factories (Hakobyan *et al.*, 2018). To assess the effect of hycanthone on the production

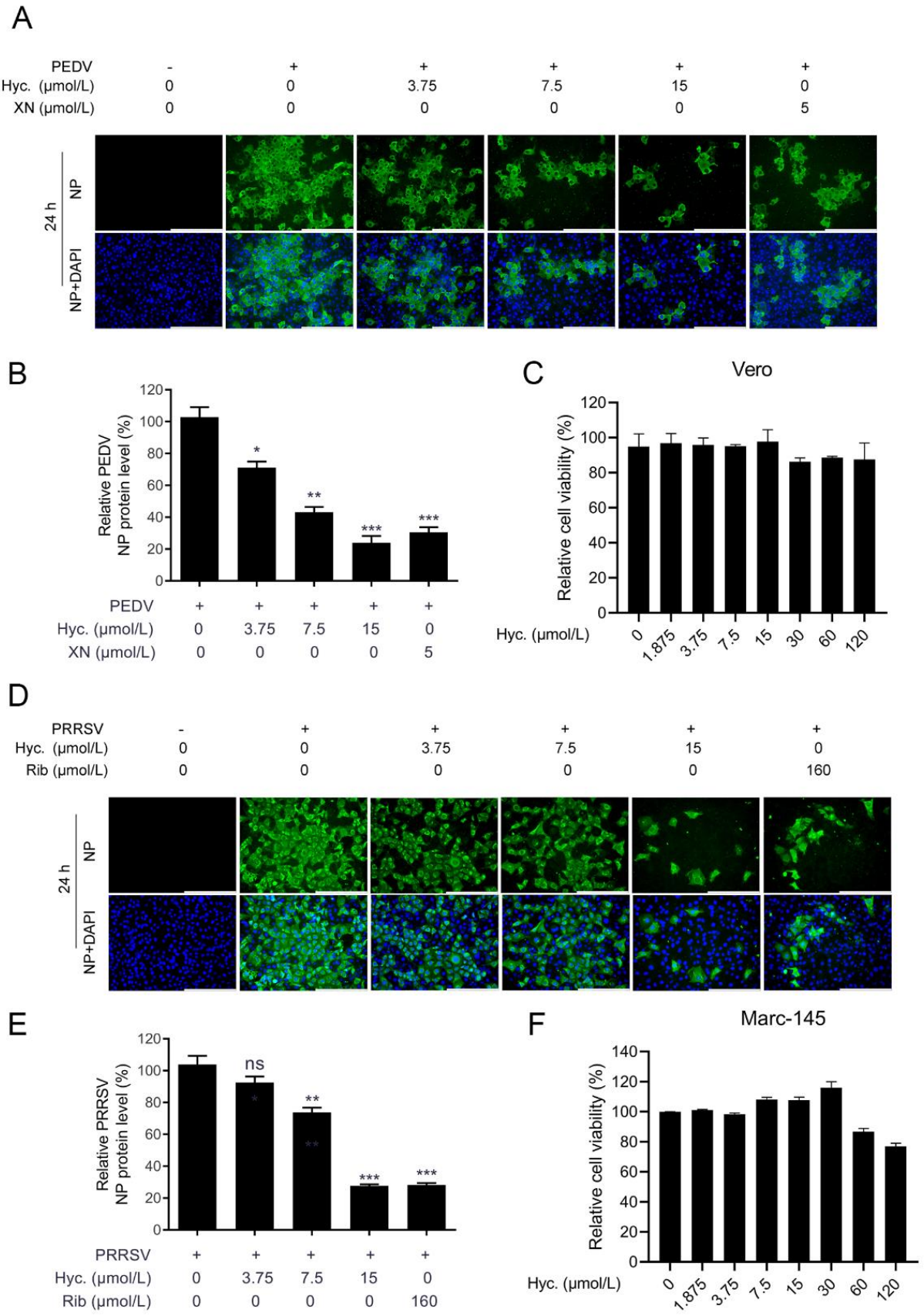

Fig. S1: Broad-spectrum antiviral activity of hycanthone against PEDV and PRRSV. (A, B, D, E) Vero or Macr-145 cells were infected with PEDV or PRRSV, respectively, for 2 h and then treated with varying concentrations of hycanthone. (A, D) The expression of NP protein for PEDV or PRRSV was analyzed by IFA, with nuclei counterstained using DAPI. Scale bar: 250 μm. (B, E) The relative NP protein levels of the viral proteins were calculated from fluorescence optical densities (OD) of the images from three independent experiments, with results expressed as percentages relative to the mock-treated controls. (C, F) Cytotoxicity of hycanthone in Vero or Macr-145 cells was evaluated by MTT assay at 24 h post-treatment, with results shown as percentages of mock-treated cells. Statistical significance is denoted by * $P<0.05$, ** $P<0.01$ and *** $P<0.001$.

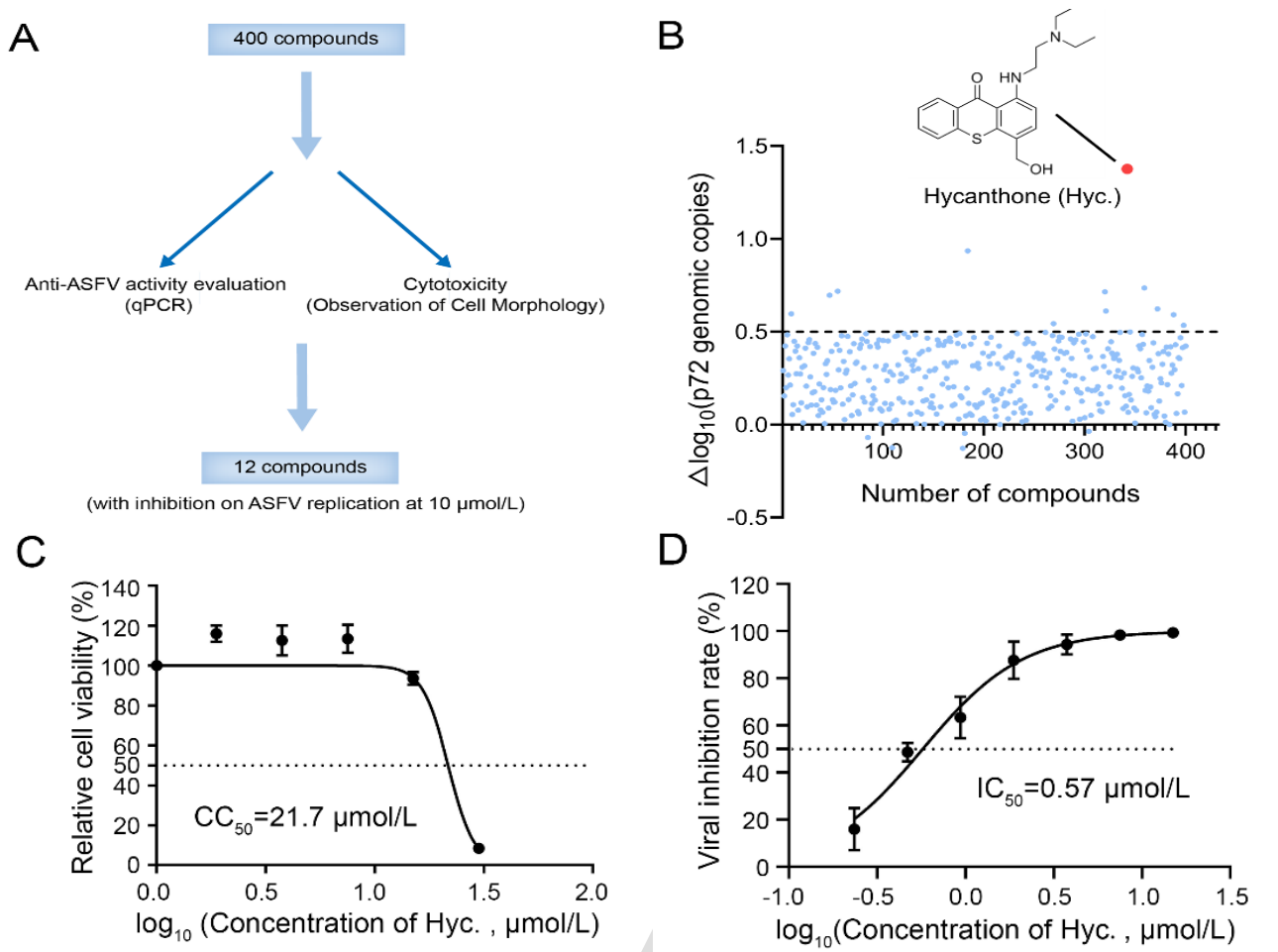

Fig. 1: Hycanthone inhibits ASFV replication in PAMs. (A) Screening flowchart for anti-ASFV compounds, illustrating the process of identifying effective compounds. (B) Inhibitory effects of various compounds (10 μM) on ASFV replication were quantified by qPCR. (C) Cytotoxicity of hycanthone was assessed in PAMs by MTT assay, with results expressed as percentages relative to mock-treated controls. (D) Dose-response curve illustrating the inhibitory effects of hycanthone on ASFV replication, with IC_{50} value calculated from viral titer titration data.

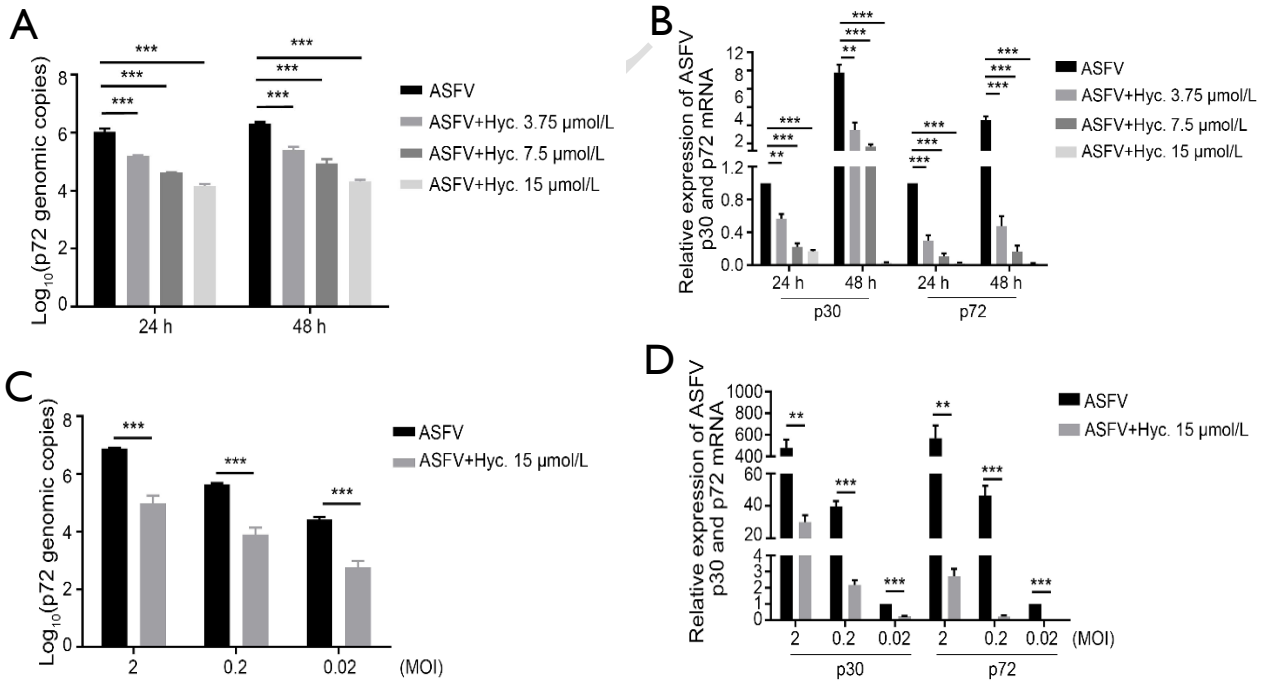

Fig. 2: Confirmation of hycanthone inhibition on ASFV replication in PAMs. PAMs were infected with ASFV (0.2 MOI) for 2 h and then treated with varying concentrations of hycanthone. (A) Viral p72 genomic copies were measured at different time points by qPCR. (B) p30 and p72 mRNA levels were quantified using RT-qPCR. (C) PAMs were infected with different ASFV MOIs (0.02, 0.2, and 2), followed by treatment with 15 μmol/L hycanthone. The viral genome and mRNA levels were measured at 24 hpi by qPCR and RT-qPCR. Statistical significance: ***P*<0.01, ****P*<0.001 vs DMSO control.

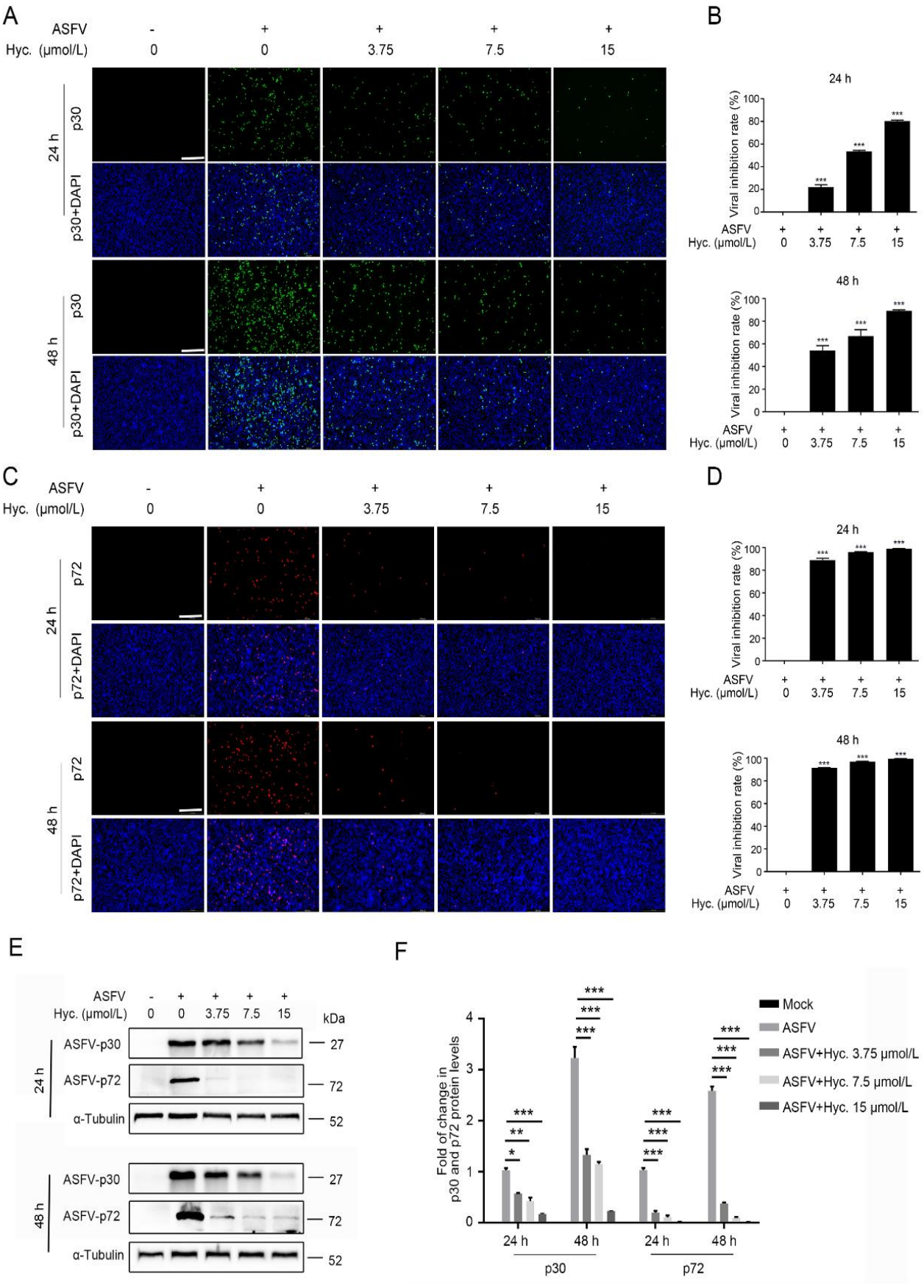

Fig. 3: Hycanthone treatment leads to reduced viral protein synthesis. PAMs were infected with ASFV (1 MOI) for 2 h and then treated with hycanthone at different concentrations. (A) p30 protein expression was analyzed by IFA, with nuclei counterstained by DAPI. (C) p72 protein expression was similarly analyzed by IFA. (B, D) Fluorescence intensities were quantified to assess viral inhibition rate. (E) Western blot analysis of p30 and p72 protein levels at 24 and 48 hpi, with α-tubulin as a loading control. (F) Densitometric analysis of p30 and p72 protein levels from three independent Western blot experiments. Scale bar: 250 μm. Statistical significance: * $P<0.05$, ** $P<0.01$ and *** $P<0.001$ vs DMSO control.

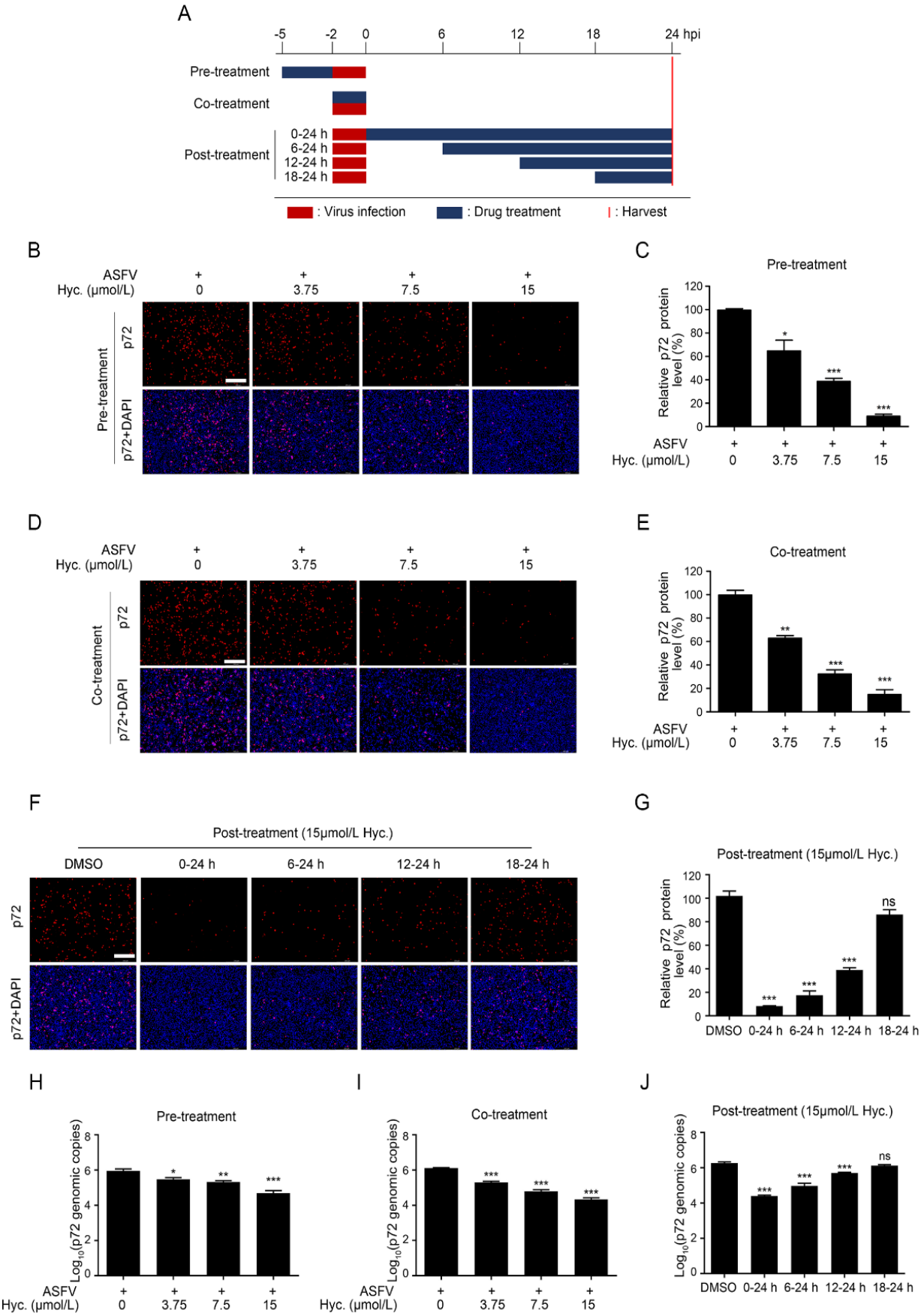

Fig. 4: Hycanthone exhibits inhibition on ASFV replication in pre-, co- and post-treatment modes. PAMs were treated with different concentrations of hycanthone in pre-, co-, or post-treatment modes. (A) Schematic representation of hycanthone treatment relative to ASFV infection, including pre-, co-, and post-treatment conditions. (B, D, F) Viral p72 protein levels were assessed by IFA, with fluorescence intensities normalized to DMSO-treated controls. (H, I, J) Viral p72 genomic copies were quantified by qPCR for each treatment condition. Scale bar: 250 μm. Statistical significance: * $P<0.05$, ** $P<0.01$ and *** $P<0.001$ vs DMSO control.

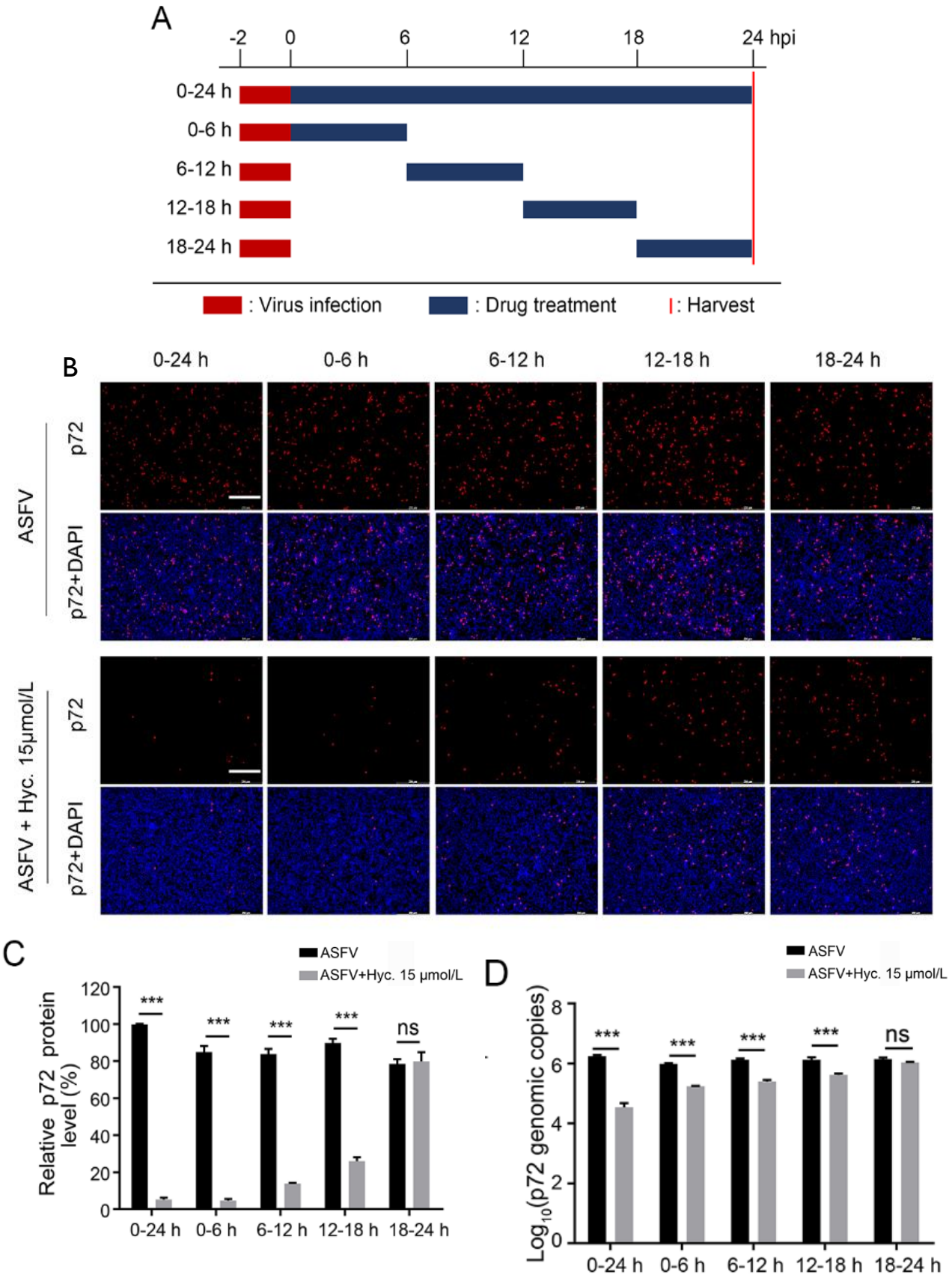

Fig. 5: Hycanthone exerts ASFV inhibition at the early and middle stages of the virus replication cycle. PAMs were infected with ASFV (1 MOI) for 2 h, followed by treatment with 15 μmol/L hycanthone during different post-infection time windows. (A) Schematic diagram of the experimental timeline showing hycanthone treatment during different post-infection intervals following ASFV infection. (B) p72 protein levels were analyzed by IFA, and fluorescence intensities were quantified (C). (D) p72 genomic copies were quantified by qPCR. Scale bar: 250 μm. Statistical significance: ***$P <$ 0.001 vs DMSO control; ns: not significant.

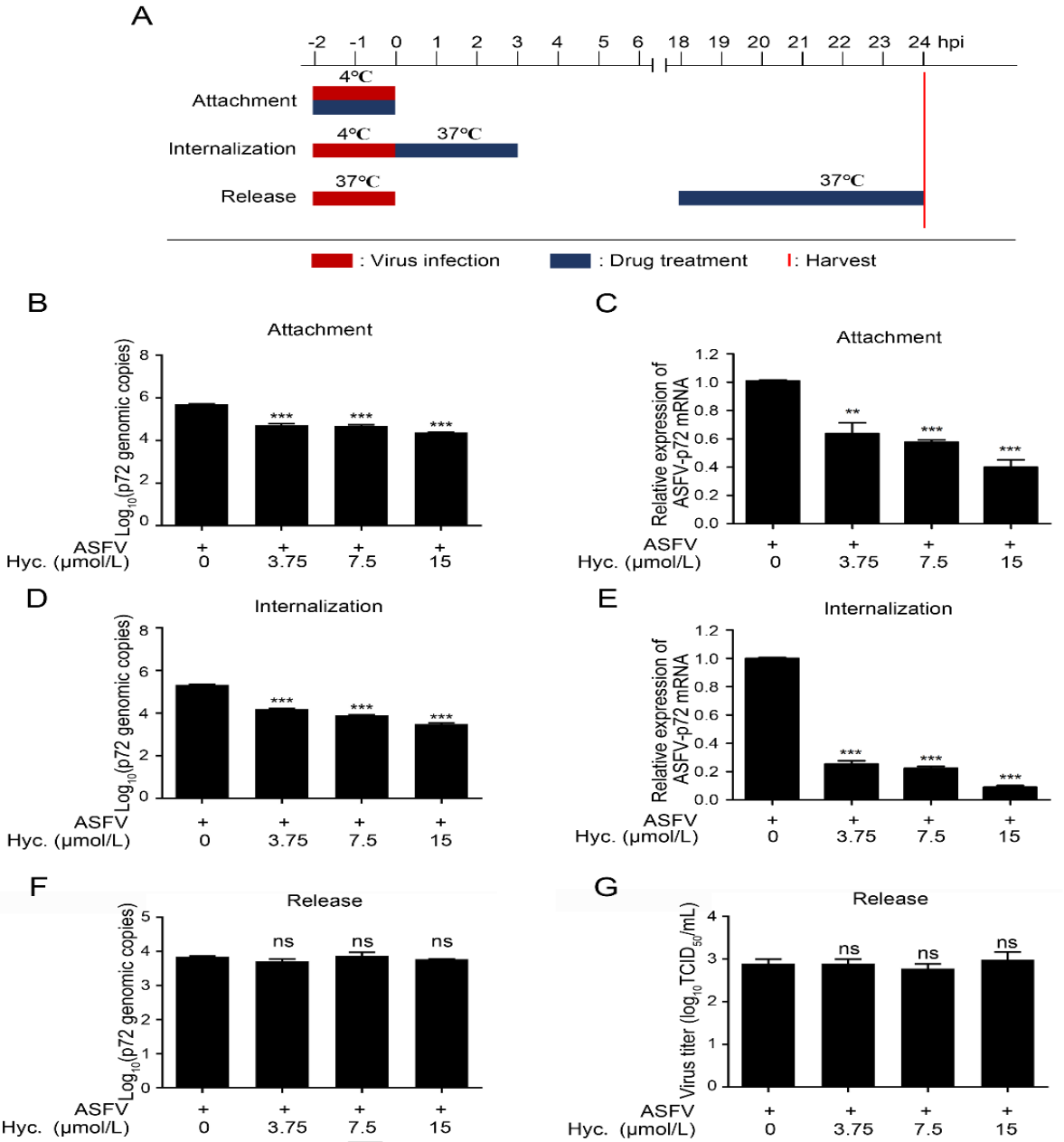

Fig. 6: Hycanthone suppresses viral attachment and internalization rather than release in PAMs. (A) Schematic representation of the experimental procedures for attachment, internalization, and release assays. (B, C) Quantification of viral p72 genomic DNA and mRNA levels by qPCR and RT-qPCR to evaluate the inhibitory effect on viral attachment. (D, E) Viral p72 genomic DNA and mRNA levels were quantified to assess internalization inhibition. (F) For release assays, viral p72 genomic copies and progeny virus titers were measured at 24 hpi. Statistical significance: $^{**}P < 0.01$, $^{***}P < 0.001$ vs DMSO control; ns: not significant.

of ASFV factories, PAMs were infected with ASFV and subsequently treated with 15 μmol/L hycanthone, and viral factory formation was quantified. Results showed that hycanthone treatment significantly reduced the number of virus factories, with an 89% decrease at 16 hpi compared with the virus control (Fig. 8A, C). Additionally, we assessed the effect of hycanthone to viral DNA integrity using a comet assay. Ara-C, a compound that indirectly exerts anti-ASFV activity by inhibiting DNA polymerase, was used as a positive control (Li *et al.*, 2024), while TSN was reported to have significant inhibition on ASFV replication through upregulating interferon regulatory factor 1 in PAMs and thus it is served as the negative control (Liu *et al.*, 2022). Comet tailing appeared in ASFV-infected PAMs treated with hycanthone and Ara-C but not in those treated with TSN or in uninfected cells (Fig. 8B, D), suggesting hycanthone induces viral DNA fragmentation. These results indicate that hycanthone causes damage to the ASFV genome.

To address genomic damage, ASFV employs a Base Excision Repair (BER) system, which is comprised by three core enzymatic components: AP endonuclease (*pE296R*), DNA polymerase X-like enzyme (*pO174L*), and DNA ligase (*pNP419L*). Molecular docking data (not shown) indicated preferential binding of hycanthone to AP endonuclease (ΔG=−6.92 kcal/mol) compared to other two BER components (DNA polymerase X-like enzyme: −4.39 kcal/mol; DNA ligase: −4.06 kcal/mol), prompting focused analysis on this interaction. As shown in Fig. 9A and 9B, hycanthone formed hydrogen bonds with amino acids CYS226 and MET240 within appropriate distance (1.89 Å and 2.06 Å, respectively) of ASFV AP endonuclease chain

A and pi-sulfur with nucleic acids MET240 of ASFV AP endonuclease chain B. Notably, LYS243 of ASFV AP endonuclease chain B forms two hydrophobic bonds (Amide-pi Stacked and pi-alkyl) with hycanthone's three cyclic structures. Thereby, we propose that hycanthone may potentially inhibit ASFV AP endonuclease activity to disrupt ASFV genome maintenance and thus interrupt the viral DNA replication.

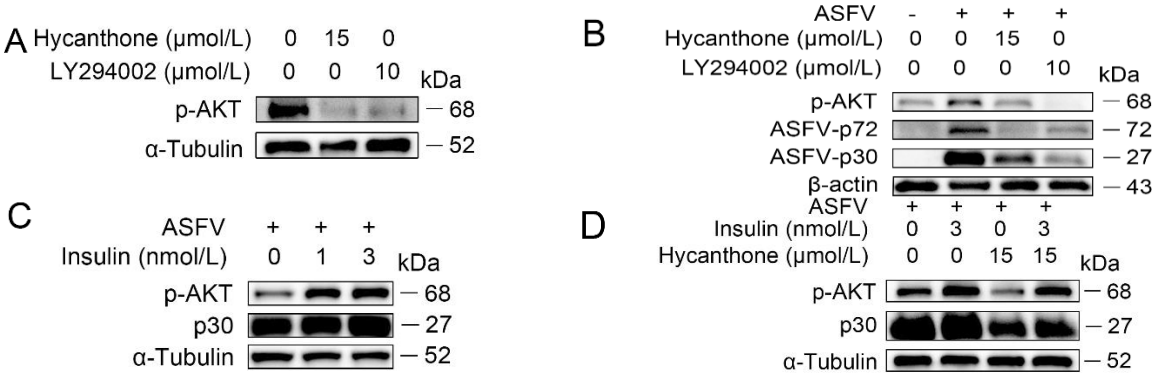

Fig. 7: Hycanthone exhibits inhibition on ASFV replication by inhibiting p-AKT expression. (A) The expression of p-AKT in PAMs treated with hycanthone or AKT inhibitor LY294002 was assessed by Western blotting. (B) Effects of hycanthone treatment on the expressions of p-AKT and viral proteins (p72 and p30). (C, D) The impact of insulin (AKT activator) and hycanthone on the expressions of p-AKT and viral p30 protein in ASFV-infected PAMs was analyzed by Western blotting.

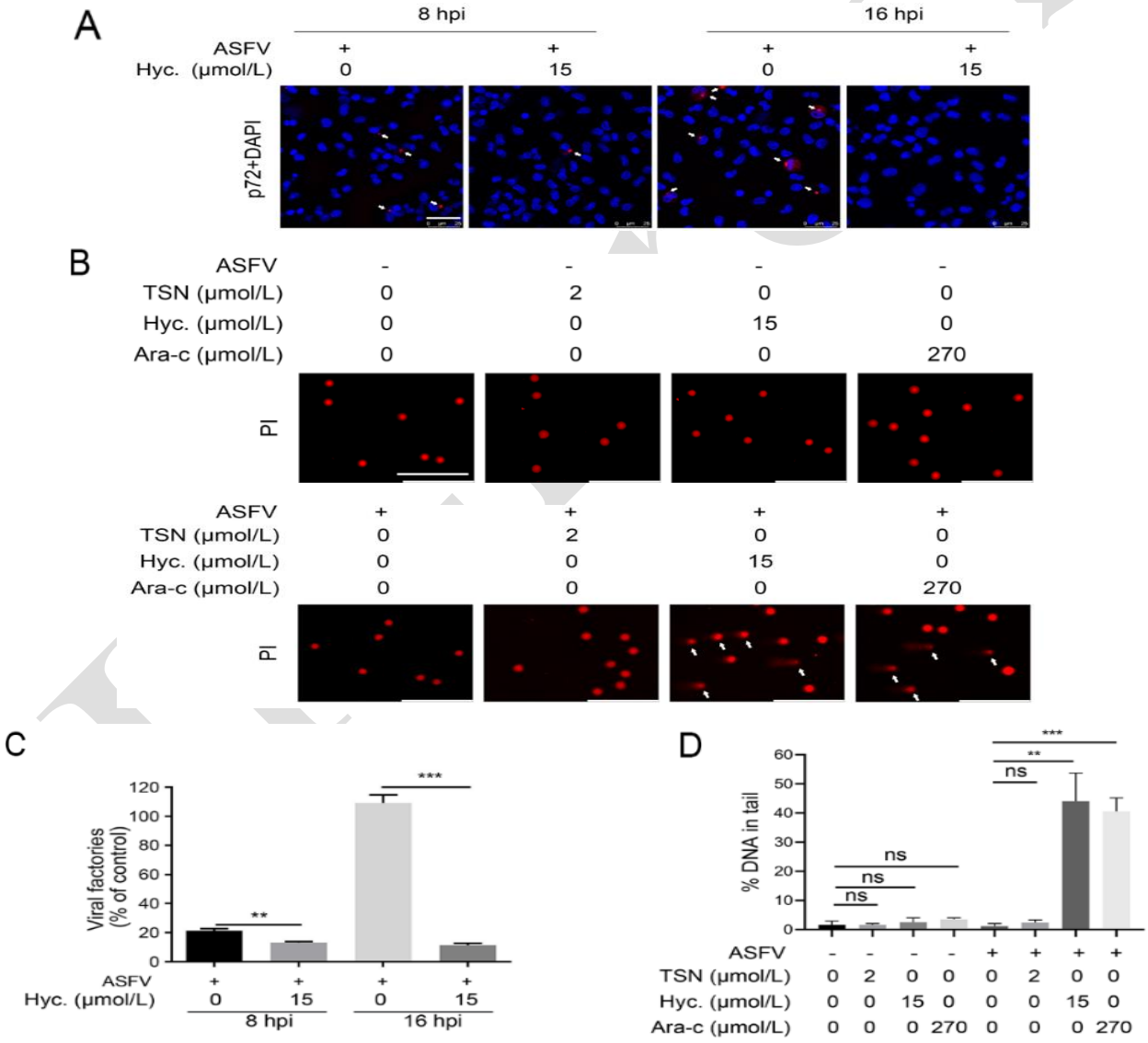

Fig. 8: Hycanthone induces the virus DNA damage. (A) Confocal microscopy was used to visualize viral factory formation in ASFV-infected PAMs with or without hycanthone treatment. (B) DNA damage was evaluated by comet assay in ASFV-infected and not infected PAMs treated with hycanthone. (C) Quantification of viral factory formation based on normalized fluorescence intensity. (D) DNA damage was assessed by calculating the percentage of DNA in comet tails. Scale bar: 250 μm. Statistical significance: $^{**}P < 0.01$, $^{***}P < 0.001$ vs DMSO control; ns: not significant.

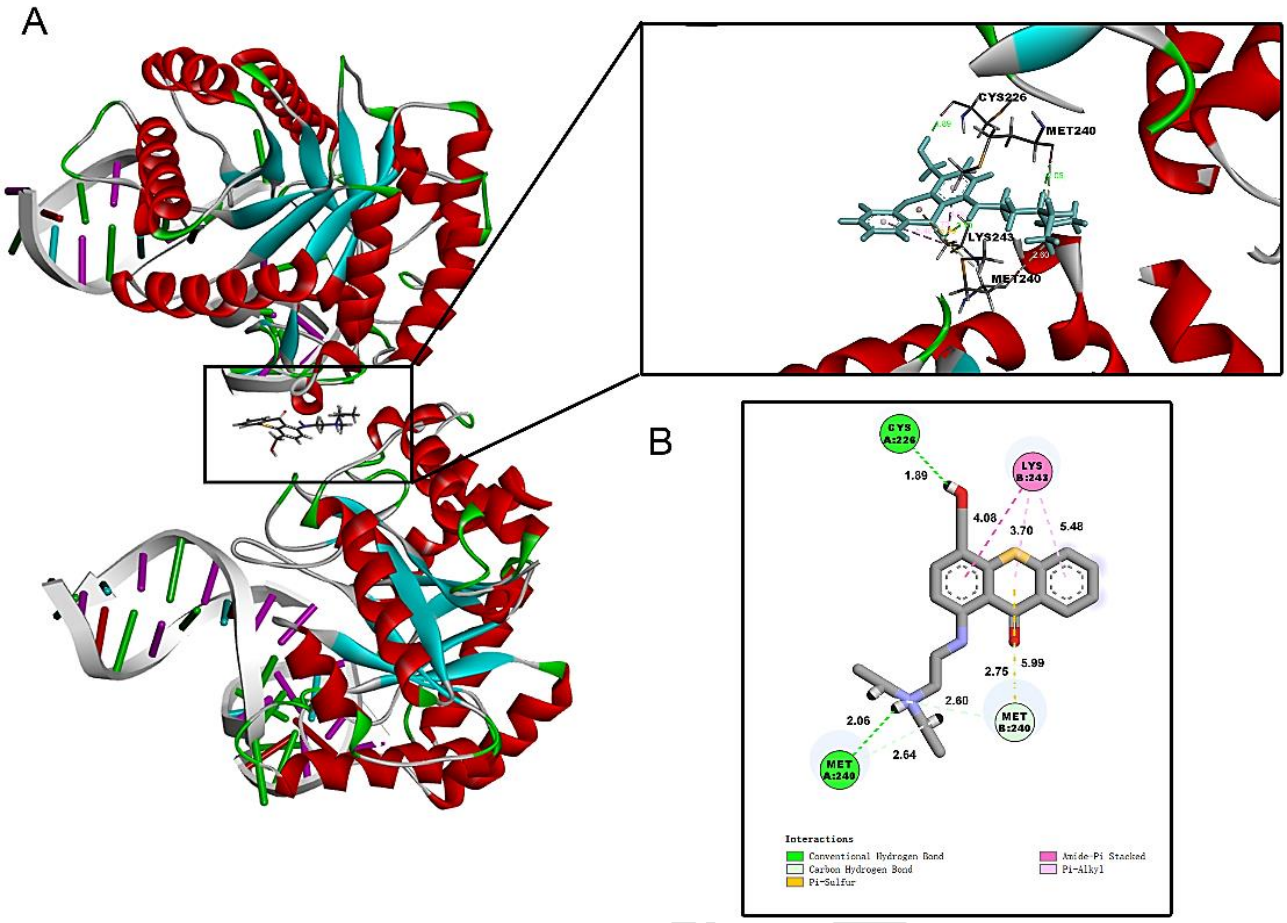

Fig. 9: Molecular model of ASFV AP endonuclease - hycanthone binding. (A) Structural schematic of ASFV AP endonuclease (PDB: 6ki3) interacting with DNA and hycanthone. (B) 2D interaction diagram showing binding sites of hycanthone (thick stick models) with ASFV AP endonuclease dimer (stick models), including hydrogen bonds, pi-sulfur interactions, amide-pi stacking, and pi-alkyl interactions.

DISCUSSION

ASFV poses a severe threat to the pig industry due to its high infectivity and mortality. Despite extensive efforts, vaccine development remains challenging. Here, we identify hycanthone, a repurposed antiparasitic agent, as a potent novel inhibitor of ASFV replication in PAMs, with submicromolar efficacy (IC_{50}=0.57 μmol/L) (Fig. 1-6). Mechanistically, hycanthone inhibits ASFV by suppressing virus-induced AKT phosphorylation (Ser473) (Fig. 7) and causing viral DNA damage (Fig. 8-9). This work represents the first report of hycanthone's antiviral activity beyond its historical role in schistosomiasis treatment via DNA alkylation (Pica-Mattoccia *et al.*, 1988).

AKT phosphorylates downstream effectors to regulate essential cellular processes, including metabolic pathways and survival signaling (Liu *et al.*, 2023). Pathogenic viruses like ASFV, PRRSV, and flaviviruses exploit the AKT pathway to enhance replication and persistence (Chang *et al.*, 2024; Palmero Casanova *et al.*, 2024; Su *et al.*, 2024). Crucially, AKT phosphorylation is essential for ASFV cellular entry, facilitating internalization via both macropinocytosis and clathrin-mediated endocytosis (S. Yang *et al.*, 2023). Our results demonstrate that hycanthone significantly inhibits ASFV attachment/internalization (Fig. 6) and suppresses virus-induced AKT phosphorylation at Ser473 (Fig. 7). Given the established role of AKT phosphorylation in ASFV entry, hycanthone's inhibition of AKT phosphorylation thus likely underlies its disruption of viral entry. However, the specific mechanism by which hycanthone suppresses AKT phosphorylation remains to be elucidated.

The complete ASFV life cycle was traditionally estimated at ~24 hours (Gaudreault *et al.*, 2020; Ruedas-Torres *et al.*, 2024). Recent studies refine this, showing viral DNA synthesis initiates at 4 hpi, peaks at 8 hpi alongside factory maturation, with progeny morphogenesis largely complete by 9 hpi (Weng *et al.*, 2025). This defines the productive replication phase within 9 hpi. Hycanthone significantly inhibited ASFV replication during this critical early window (0-12 h; Fig. 5), reducing viral factory formation (Fig. 8A) and compromising viral genome integrity (Fig. 8B), indicating impaired DNA replication.

ASFV infection elevates ROS in PAMs, causing oxidative DNA damage that impairs replication (Liu *et al.*, 2025). To counteract such genotoxic stress, ASFV encodes a dedicated BER pathway, composed of three key enzymatic components: (1) AP endonuclease (pE296R), which recognizes and cleaves DNA at AP sites created by oxidative or alkylative damage; (2) a DNA polymerase X-like enzyme (pO174L), which fills in the single-nucleotide gap following cleavage; and (3) a DNA ligase (pNP419L), which seals the nick to complete the repair process (Chen *et al.*, 2022). Molecular docking revealed hycanthone's strongest binding affinity for the viral AP endonuclease (pE296R; ΔG=−6.92 kcal/mol) versus other BER enzymes (Fig. 9). Given pE296R's essential role and upregulation at

2-6 hpi (Redrejo-Rodriguez *et al.*, 2006), hycanthone likely inhibits AP endonuclease-mediated repair of oxidative DNA lesions, compromising viral genome maintenance under ROS stress. However, functional confirmation of the interaction of hycanthone with the viral AP, including the enzymatic inhibition assay, remains to be investigated.

A key concern in targeting DNA repair enzymes is the potential off-target impact on host cell functions. In mammalian cells, APE1 is the primary AP endonuclease, playing vital roles in DNA repair, redox homeostasis, transcriptional regulation, and cell cycle control (Manoel-Caetano et al., 2020; Siqueira et al., 2024). However, sequence alignment shows only ~20% identity between ASFV AP endonuclease and porcine APE1, with non-conserved residues at hycanthone's binding sites, suggesting structural divergence favors viral targeting. This is supported by its closer homology to mimivirus endonuclease IV than host APE1 (Redrejo-Rodriguez *et al.*, 2006). Further biophysical validation (ITC, SPR, crystallography) is warranted to confirm selectivity.

Although hycanthone use in pigs remains unreported, pharmacokinetic studies in rhesus monkeys demonstrate that intramuscular administration (3 mg/kg) achieves peak plasma concentrations (~0.65 μg/mL or 1.83 μmol/L) within 30 minutes (Hernandez *et al.*, 1971). This concentration is threefold higher than its *in vitro* anti-ASFV IC_{50} (0.57 μmol/L), supporting its potential to reach efficacious levels *in vivo*. Additionally, we observed that hycanthone inhibits the replication of two other porcine viruses, PRRSV and PEDV (Fig. S1) in Marc-145 and Vero cells, respectively, suggesting its broad-spectrum antiviral potential against pig diseases.

In conclusion, we present the first evidence that hycanthone inhibits ASFV replication. The compound exerts its antiviral effect by inhibiting the cellular AKT phosphorylation and inducing viral DNA damage, thereby disrupting viral DNA replication. These findings expand our understanding of hycanthone's potential as an anti-ASFV agent, though further studies are needed to evaluate its *in vivo* efficacy in pigs.

Authors' contributions: ZL and YL conceptualized the study and designed the research framework. ZL, GS, HL and WO performed experiments and collected the data. ZL conducted formal data analysis, including statistical analysis and visualization. JC secured funding acquisition and provided project administration. ZL wrote the original draft of the manuscript. WC and JC reviewed and edited the manuscript, providing critical feedback and revisions. LH and CW contributed essential experimental materials and resources. All authors reviewed and approved the final version of the manuscript.

Funding: This research was funded by the National Natural Science Foundation of China (Grant No. 31941019), and the National Key Research and Development Program of China (Grant No. 2022YFD1802103).

Availability of data and materials: All the data contained within this manuscript.

Conflicts of interest: All Authors declare no conflict of interest.

REFERENCES

Arabyan E, Hakobyan A, Kotsinyan A, *et al.*, 2018. Genistein inhibits African swine fever virus replication in vitro by disrupting viral DNA synthesis. Antiviral Res 156:128-137.

Bases RE, Mendez F, 1997. Topoisomerase inhibition by lucanthone, an adjuvant in radiation therapy. Int J Radiat Oncol Biol Phys 37:1133-1137.

Boo KJ, Gonzales EL, Remonde CG, *et al.*, 2023. Hycanthone inhibits inflammasome activation and neuroinflammation-induced depression-like behaviors in mice. Biomol Ther 31:161-167.

Chang K, Fan K, Zhang H, *et al.*, 2024. Fuzhengjiedu San inhibits porcine reproductive and respiratory syndrome virus by activating the PI3K/AKT pathway. PLoS One 19:e0283728.

Chen H, Wang Z, Gao X, *et al.*, 2022. ASFV pD345L protein negatively regulates NF-κB signalling by inhibiting IKK kinase activity. Vet Res 53:32.

Chen Y, Song Z, Chang H, *et al.*, 2023. Dihydromyricetin inhibits African swine fever virus replication by downregulating toll-like receptor 4-dependent pyroptosis in vitro. Vet Res 54:58.

Freitas FB, Frouco G, Martins C, *et al.*, 2016. In vitro inhibition of African swine fever virus-topoisomerase II disrupts viral replication. Antiviral Res 134:34-41.

Galindo I, Hernáez B, Berná J, *et al.*, 2011. Comparative inhibitory activity of the stilbenes resveratrol and oxyresveratrol on African swine fever virus replication. Antiviral Res 91:57-63.

Gaudreault NN, Madden DW, Wilson WC, *et al.*, 2020. African swine fever virus: an emerging DNA arbovirus. Front Vet Sci 7:215.

Grigoryan R, Arabyan E, Izmailyan R, *et al.*, 2022. Antiviral activity of brequinar against African swine fever virus infection in vitro. Virus Res 317:198826.

Hakobyan A, Arabyan E, Kotsinyan A, *et al.*, 2019. Inhibition of African swine fever virus infection by genkwanin. Antiviral Res 167:78-82.

Hakobyan A, Galindo I, Nanez A, *et al.*, 2018. Rigid amphipathic fusion inhibitors demonstrate antiviral activity against African swine fever virus. J Gen Virol 99:148-156.

Han Y, Zhang Z, Yang H, *et al.*, 2024. Protective effects of SHLO on LPS-induced lung injury via TLR4/Myd88-ERK signaling pathway and intestinal flora regulation. Pak Vet J 44:776-784.

Hernandez P, Dennis EW, Farah A, 1971. Metabolism of the schistosomicidal agent hycanthone by rats and rhesus monkeys. Bull World Health Organ 45:27-34.

Li L, Fu J, Li J, *et al.*, 2022. African swine fever virus pI215L inhibits type I interferon signaling by targeting interferon regulatory factor 9 for autophagic degradation. J Virol 96:e0094422.

Li T, Zheng J, Huang T, *et al.*, 2024. Identification of several African swine fever virus replication inhibitors by screening of a library of FDA-approved drugs. Virology 593:110014.

Li X, Han YR, Xuefeng X, *et al.*, 2022. Lentivirus-mediated short hairpin RNA interference of CENPK inhibits growth of colorectal cancer cells with overexpression of Cullin 4A. World J Gastroenterol 28:5420-5443.

Lim KB, Kim DH, Kim JH, *et al.*, 2024. Evaluation of antiviral efficacy of recombinant feline interferon lambda-1 against calicivirus. Pak Vet J 44:1269-1274.

Liu D, Li LF, Zhai H, *et al.*, 2025. Resveratrol inhibits African swine fever virus replication via the Nrf2-mediated reduced glutathione and antioxidative activities. Emerg Microbes Infect 14:2469662.

Liu Y, Kong H, Cai H, *et al.*, 2023. Progression of the PI3K/Akt signaling pathway in chronic obstructive pulmonary disease. Front Pharmacol 14:1238782.

Liu Y, Li Y, Xie Z, *et al.*, 2021. Development and in vivo evaluation of MGF100-1R deletion mutant in an African swine fever virus Chinese strain. Vet Microbiol 261:109208.

Liu Y, Zhang X, Liu Z, *et al.*, 2022. Toosendanin suppresses African swine fever virus replication through upregulating interferon regulatory factor 1 in porcine alveolar macrophage cultures. Front Microbiol 13:970501.

Nuanualsuwan S, Songkasupa T, Boonpornprasert P, *et al.*, 2022. Thermal inactivation of African swine fever virus in swill. Front Vet Sci 9:906064.

Palmero Casanova B, Albentosa González L, Maringer K, *et al.*, 2024. A conserved role for AKT in the replication of emerging flaviviruses in vertebrates and vectors. Virus Res 348:199447.

Pica-Mattoccia L, Cioli D, Archer S, 1988. Binding of tritiated hycanthone and hycanthone N-methylcarbamate to macromolecules of drug-

sensitive and drug-resistant schistosomes. Mol Biochem Parasitol 31:87-96.

Redrejo-Rodriguez M, Garcia-Escudero R, Yanez-Munoz RJ, *et al.*, 2006. African swine fever virus protein pE296R is a DNA repair apurinic/apyrimidinic endonuclease required for virus growth in swine macrophages. J Virol 80:4847-4857.

Ruedas-Torres I, Thi To Nga B, Salguero FJ, 2024. Pathogenicity and virulence of African swine fever virus. Virulence 15:2375550.

Salas ML, Andres G, 2013. African swine fever virus morphogenesis. Virus Res 173:29-41.

Su G, Yang X, Lin Q, *et al.*, 2024. Fangchinoline inhibits African swine fever virus replication by suppressing the AKT/mTOR/NF-κB signaling pathway in porcine alveolar macrophages. Int J Mol Sci 25:7178.

Varbanov HP, Kuttler F, Banfi D, *et al.*, 2019. Screening-based approach to discover effective platinum-based chemotherapies for cancers with poor prognosis. PLoS One 14:e0211268.

Wang C, Guo B, Yang Z, *et al.*, 2023. Discovery of novel hybrid-type strigolactone mimics derived from cinnamic amide. Int J Mol Sci 24:9967.

Warren KS, Siongok TK, Ouma JH, *et al.*, 1978. Hycanthone dose-response in Schistosoma mansoni infection in Kenya. Lancet 1:352-354.

Weng W, Wang H, Ye M, *et al.*, 2025. Revisiting the early event of African swine fever virus DNA replication. J Virol 99:e0058425.

Yang B, Hao Y, Yang J, *et al.*, 2023. PI3K-Akt pathway-independent PIK3AP1 identified as a replication inhibitor of the African swine fever virus based on iTRAQ proteomic analysis. Virus Res 327:199052.

Yang S, Miao C, Liu W, *et al.*, 2023. Structure and function of African swine fever virus proteins: Current understanding. Front Microbiol 14:1043129.

Zhou P, Li LF, Zhang K, *et al.*, 2022. Deletion of the H240R gene of African swine fever virus decreases infectious progeny virus production due to aberrant virion morphogenesis and enhances inflammatory cytokine expression in porcine macrophages. J Virol 96:e0166721.